FEBS Open Bio 3 (2013) 130–134

journal homepage: www.elsevier.com/locate/febsopenbio

# Atrophy of myoepithelial cells in parotid glands of diabetic mice; detection using skeletal muscle actin, a novel marker☆

Tomoko Nashida[a,*], Sumio Yoshie[b], Maiko Haga-Tsujimura[b], Akane Imai[a], Hiromi Shimomura[a]

[a]Department of Biochemistry, The Nippon Dental University, School of Life Dentistry at Niigata, 1-8 Hamaura-cho, Chuo-ku, Niigata 951-8580, Japan
[b]Department of Histology, The Nippon Dental University, School of Life Dentistry at Niigata, 1-8 Hamaura-cho, Chuo-ku, Niigata 951-8580, Japan

ARTICLE INFO

*Article history:*
Received 5 December 2012
Received in revised form 22 January 2013
Accepted 25 January 2013

*Keywords:*
Myoepithelial cells
Skeletal muscle actin
Parotid gland
Diabetic NOD mouse

ABSTRACT

**In mouse parotid glands, we found expression of skeletal muscle actin (actin-α1) protein and mRNA. We isolated myoepithelial cells from the mouse parotid glands and investigated their actin-α1 expression because smooth muscle actin (actin-α2) has been used as a marker for myoepithelial cells. We used actin-α1 expression to identify pathological changes in diabetic non-obese diabetic (NOD; NOD/ShiJcl) mice—a mouse model for Sjögren's syndrome—and found myoepithelial cells to be decreased or atrophied in the diabetic state.**



## 1. Introduction

Myoepithelial cells have been found in association with intercalated ducts and with acini in all mammalian salivary glands [1]. Myoepithelial cells have been thought to be contractile because their fine structures are similar to those of smooth muscle [2]. Smooth muscle-specific actin (actin-α2), cytokeratin 14 and S100 protein have been used as markers of myoepithelial cells in histogenetic studies of salivary gland tumors [1,2], although these markers are not specific for salivary gland myoepithelial cells because of the number of capillary vessels in the glands.

Non-obese diabetic (NOD) mice develop salivary glands hypofunction and are commonly used to study autoimmune diabetes [3]. Salivary glands of NOD mice are histologically similar to salivary glands of patients with Sjögren's syndrome, and are thus useful as a model for this disease [4,5]. We previously investigated differential gene expression in parotid glands of diabetic NOD mice, using a cDNA microarray assay, and found that the interspace between acinar cells was extended in diabetic mice [6]; we also found that some genes, including those for aquaporin 8 (*Aqp8*) and skeletal muscle actin-α (*Acta1*), were expressed less in diabetic NOD mice than in non-diabetic NOD mice and controls. As aquaporin 8 expression in parotid gland myoepithelial cells has been reported previously [7], we supposed that myoepithelial cells might decrease or shrink as diabetes develops, and myoepithelial cells might express skeletal muscle actin (actin-α1), although expression of skeletal muscle actin in the myoepithelial cells has not been reported.

Therefore, to clarify the pathogenesis of parotid glands in Sjögren's syndrome using this mouse model, we investigated the decrease in myoepithelial cells in parotid glands of diabetic and non-diabetic NOD mice, and in control mice. We also studied expression of actin-α1 in parotid myoepithelial cells, and its potential as a novel marker for myoepithelial cells.

## 2. Materials and methods

### 2.1. Materials

Mouse monoclonal antibody specific for aquaporin 8 (M01) was purchased from Abnova (Taipei, Taiwan). Rabbit polyclonal antibody specific for aquaporin 5 was obtained from Millipore (Billerica, MA, USA). Rabbit polyclonal antibody specific for actin-α1 was obtained from Bioworld Technology (Minneapolis, MN, USA), and rabbit polyclonal antibody specific for actin-α2 was from Gene Tex Inc. (San Antonio, TX, USA). Alexa-Fluor 555 phalloidin was obtained from Molecular Probes (Eugene, OR, USA). DAPI (4′,6-diamidino-2-phenylindole) was obtained from Dojindo (Kumamoto, Japan).

### 2.2. Animals

All procedures were conducted to minimize pain and discomfort according to the Guidelines for the Care and Use of Laboratory Animals, The Nippon Dental University, School of Life Dentistry at Niigata. Female mice were bred and maintained under special pathogen-free



* Corresponding author. Tel.: +81 25 267 1500x592; fax: +81 25 267 1134.
*E-mail address:* nashida@ngt.ndu.ac.jp (T. Nashida).

2211-5463/$36.00 
http://dx.doi.org/10.1016/j.fob.2013.01.009

conditions in the mouse facility of our university. For the investigation of diabetic mice, female NOD/ShiJcl and C57BL/6JJcl mice (10 weeks old) were purchased from Clea Japan Inc. (Tokyo, Japan) and housed in an environmentally controlled room (12-h light–dark cycle, 23 ± 3 °C and 50 ± 20% relative humidity). The animals had *ad libitum* access to certified rodent chow (Oriental Yeast, Tokyo, Japan) and water, and were acclimatized under these conditions. Mice were tested for blood glucose levels using OneTouch Ultra Test Strips (Life Scan Inc., Milpitas, CA, USA). Consecutive elevated fasting blood glucose levels >240 mg/dl were considered to represent the onset of diabetes. NOD mice between 25 and 28 weeks of age were separated into diabetic and non-diabetic groups (12 animals each), and were used for experiments, with C57BL/6JJcl mice (12 animals) at 25 weeks as the control group. For the investigation of actin-α1 in myoepithelial cells, Slc:ICR mice (Japan SLC, Inc., Hamamatsu, Japan) at 10 weeks were used.

### 2.3. Preparation of homogenates from parotid glands

To obtain three individual samples from each group, minced parotid glands from a mouse were homogenized with ice-cold buffer containing 5 mM HEPES–NaOH (pH 7.5), 50 mM mannitol, 0.25 mM $MgCl_2$, 25 mM β-mercaptoethanol, 0.1 mM ethyleneglycol-bis (2-aminoethyl ether) *N*,*N*,*N*′,*N*′-tetra acetic acid (EGTA), 2 mM leupeptin, 2.5 μg/ml trypsin inhibitor, 0.1 mM 4-amidinophenyl methane sulfonyl fluoride hydrochloride, 5 mM benzamidine and 2 mg/ml aprotinin, using a glass homogenizer and a Teflon pestle. The mixture was then centrifuged at 500*g* for 10 min at 4 °C, and the supernatant was collected as a homogenate.

### 2.4. Isolation of acinar cells and myoepithelial cells from mouse parotid glands

Mice were anesthetized by intra-peritoneal injection of sodium pentobarbital (50 mg/kg) and sacrificed by cardiac puncture. Parotid glands were digested with collagenase (0.2 U/ml medium) for 20 min after digestion with trypsin as described previously [8]. The digest was centrifuged at 160*g* for 1 min; the precipitated layer contained acinar cells and myoepithelial cells. A mixture of 65% RediGrad in 2 mM EDTA in HBSS without $Ca^{2+}$ or $Mg^{2+}$ containing 0.1% bovine serum albumin (BSA) was pre-centrifuged at 48,000*g* for 1 h at 1 °C. The cell precipitate was added on top of the RediGrad mixture and centrifuged at 3000*g* for 10 min to obtain two fractions. The higher-density fraction came from the acinar cells, as identified by immunoblotting and immunohistochemistry [9]; the lower-density fraction came from the myoepithelial cells.

### 2.4. Immunoblotting

Samples were solubilized in Laemmli sample buffer, boiled and subjected to SDS–polyacrylamide gel electrophoresis (PAGE) using pre-made 5–20% polyacrylamide gel plates (e-PAGEL, Atto, Tokyo, Japan). The separated proteins were electrotransferred from the gel to an Immun-Blot PVDF membrane (Bio-Rad Laboratories, Hercules, CA, USA). The blots were probed with primary antibodies; immune complexes were detected with HRP-conjugated secondary antibodies and ECL plus reagents (GE Healthcare, Little Chalfont, UK), and visualized using X-OMAT film (Kodak, Rochester, NY, USA). The intensity of the immunoreactive bands on the films was quantified using the Image Gauze function of the LAS-1000 software package (Fuji Film, Tokyo, Japan).

### 2.5. Extraction of total RNA

Parotid glands or cell fractions from the parotid glands were washed with PBS, soaked in 500 μl RNA later (Life Technologies, Carlsbad, CA, USA), and stored at 4 °C overnight. Total RNA was prepared using an RNeasy Plus Mini Kit (Qiagen, Chatsworth, CA, USA) with a DNA deletion column according to the manufacturer's instructions.

### 2.6. RT-PCR analysis

First-strand complementary DNA was synthesized from 5 μg of total RNA template using Transcriptor First Strand cDNA Synthesis Kit (Roche Diagnostics, Mannheim, Germany) with oligo dT primers according to the manufacturer's instructions. Primer sets used were: *Actb* (actin-β) sense: 5′-AGCCATGTACGTAGCCATCC-3′, antisense: 5′-CTCTCAGCTGTGGTGGTGAA-3′; *Aqp5* (aquaporin 5) sense: 5′-CGAAGAGTTTGGAGCACCTC-3′, antisense: 5′-TGGTCCTGAACTGCTGTGAG-3′; *Aqp8* (aquaporin 8) sense: 5′-GCAGGACCTGAGCTAAGAGG-3′, antisense: 5′-GCATTCTCCACCTTCTCAGC-3′; *Acta1* (actin-α1) sense: 5′-CGAGGTATCCTGACCCTGAA-3′, antisense: 5′-GAAGGAATAGCCACGCTCAG-3′; and *Acta2* (actin-α2) sense: 5′-CTGACAGAGGCACCACTGAA-3′, antisense: 5′-CATCTCCTGAGTCCAGCACA-3′. PCR reactions were performed using 1 unit of KOD-Plus DNA polymerase (Toyobo, Tokyo, Japan). Amplification was performed in an Applied Biosystems 2720 Thermal Cycler (Life Technologies) with 35 cycles of the following thermal profile: 94 °C for 20 s, 60 °C for 30 s, 68 °C for 1 min. Amplified fragments were separated on a 1.8% agarose gel and detected with SYBR Green I (Lonza, Rockland, ME, USA).

### 2.7. Real-time quantitative PCR

The quantitative PCR assay was performed using TaqMan probes selected from the Universal ProbeLibrary (Roche Diagnostics) and the LightCycler (Roche Diagnostics), according to the manufacturer's instructions. Selection of TaqMan probes and primer design were performed at the Universal ProbeLibrary Assay Design Center Website. The primer sets used were: *Acta1* (NM_009606.2) sense: 5′-AATGAGCGTTTCCGTTGC-3′, antisense: 5′-ATCCCCGCAGACTCCATAC-3′; *Acta2* (NM_007392.2) sense: 5′-CTCTCTTCCAGCCATCTTTCAT-3′, antisense: 5′-TATAGGTGGTTTCGTGGATGC-3′; and *Actb* (NM_007393) sense: 5′-CTAAGGCCAACCGTGAAAAG-3′, antisense: 5′-ACCAGAGGCATACAGGGACA-3′. Transcript copy numbers of target genes were calculated using amplicons: *Acta1* 804–920 fragment, *Acta2* 816–980 fragment, and *Actb* 371–534 fragment. Copy numbers were corrected using *Actb* as an internal standard.

### 2.8. Immunocytochemistry

Parotid glands and parotid acinar cells were fixed with 4% paraformaldehyde. Fixed specimens were then rapidly frozen at −35 °C, and cut into 6-μm slices. For anti-aquaporin 8, parotid glands were rapidly frozen in precooled isopentane, cut into 8-μm-thick slices on a cryostat, mounted on slides and immersed in 4% paraformaldehyde. Individual semi-thin sections were incubated overnight with anti-aquaporin-8 (dilution 1:500), anti-aquaporin-5 (1:500), anti-actin-α2 (1:500), or anti-actin-α1 (1:500) antibody. After incubation and washing steps, these sections were exposed to fluorescent dye-conjugated secondary antibody (1:299). Immunocytochemistry of acinar cells with myoepithelial cells, and isolated myoepithelial cells described above, was performed; cells fixed with 4% paraformaldehyde were incubated with anti-aquaporin 8 and anti-actin-α1 antibodies following exposure to fluorescent dye-conjugated secondary antibodies as described above. Alexa-Fluor 555 phalloidin and DAPI were used to stain actin filaments and nuclei, respectively. Stained sections or cells were examined and photographed under a confocal laser scanning microscope (LSM 710; Zeiss, Oberkochen, Germany).

### 2.9. Statistical analysis

Data were analyzed using unpaired Student's *t*-tests to assess differences. $P < 0.05$ was considered statistically significant.

## 3. Results

### 3.1. Identification of myoepithelial cells in mouse parotid glands

Myoepithelial cells are located on the basal surface of acini and ductal cells as a thin layer, and have star-shaped morphology. Immunocytochemistry was performed on mouse parotid glands with antibodies against actin-α2 (smooth muscle protein which has been used as a marker for myoepithelial cells), aquaporin 8 (expression of which in myoepithelial cells has been reported previously [7]), and actin-α1 which has not been examined. Myoepithelial cells in parotid glands were immunoreactive to anti-actin-α1 antibody, as well as the other antibodies (Fig. 1). To certify the results, we separated myoepithelial cells from the parotid glands; parotid glands were dispersed with collagenase after trypsin treatment; the precipitate obtained by centrifugation at 160*g* from the enzyme digests included acinar cells bound to myoepithelial cells (Fig. 2A). To separate myoepithelial cells from acinar cells, the fraction was treated with 2 mM EDTA following density gradient centrifugation. The high density fraction contained the acinar cells, as determined by RT-PCR (Fig. 2D) and the micrograph (data not shown). Immunocytochemistry of the low-density fraction showed that cells included in the fraction were immunoreactive both to anti-aquaporin 8 and anti-actin-α1 antibodies (Fig. 2B). As these cells tended to be round, unlike the typical shape of myoepithelial cells, we found their original shapes by the gradient-density centrifugation after sonicating the prefixed myoepithelial cell-bound acinar cells. The cells were then confirmed as myoepithelial cells by their shape (Fig. 2C). RT-PCR of these fractions showed expression of *Aqp8*, *Acta2* and *Acta1* in the MEC fraction, but little expression of *Aqp5*—a marker for acinar cells (Fig. 2D). These indicated that this skeletal muscle component was specifically expressed in myoepithelial cells in parotid glands, and actin-α1 could be a marker for myoepithelial cells.

### 3.2. Use of actin-α1 expression to detect pathogenesis of parotid glands of NOD mice

At 28 weeks of age, NOD mice were separated and housed into two groups—diabetic and non-diabetic; the latter was recognized as a pre-diabetic group, because both might have the same autoimmune characters as defined previously [3,5]. Comparative experiments used four mice in each group. First, we compared expression of aquaporins 5 and 8 in parotid glands among the mouse groups (Fig. 3A, upper). Aquaporin 5 expression was similar, but that of aquaporin 8 was less in the diabetic NOD mice. The extracellular area stained by phalloidin (actin filaments) was also smaller in diabetic NOD mice (Fig. 3A, lower). Expression of aquaporin 8, actin-α1 and actin-α2 was less in diabetic NOD mice, but that of aquaporin 5 was similar (Fig. 3B). Decreased mRNA expression of *Aqp8*, *Aqp1* and *Aqp2* was also seen (Fig. 3C). Quantitative real-time PCR was used to study reduced gene expression in the diabetic NOD mice (Fig. 4). Relative expression of both *Acta1* and *Acta2* to the internal standard *Actb* was lower in the diabetic NOD mice than in control mice.

## 4. Discussion

Although myoepithelial cells have been isolated from, and their function identified in, mammary glands [10,11], those in salivary glands have not been isolated. Myoepithelial cells surround ductal and acinar cells in salivary glands, and they reportedly support acinar and ductal cells [12], and support stimulation of saliva secretion by

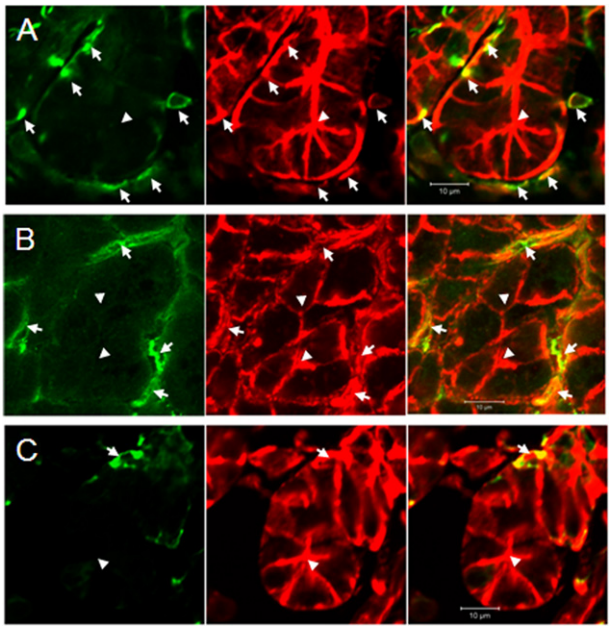


**Fig. 1.** Detection of marker proteins for myoepithelial cell in parotid glands. (Left) Immunocytochemistry with anti-actin-α2 (A), anti-aquaporin 8 (B) and anti-actin-α1 (C) antibodies in the region around acinar cells. (Right) Merged images of panels A–C and phalloidin-stained image (middle). Arrowheads indicate lumens of acinar cells; arrows indicate myoepithelial cells.

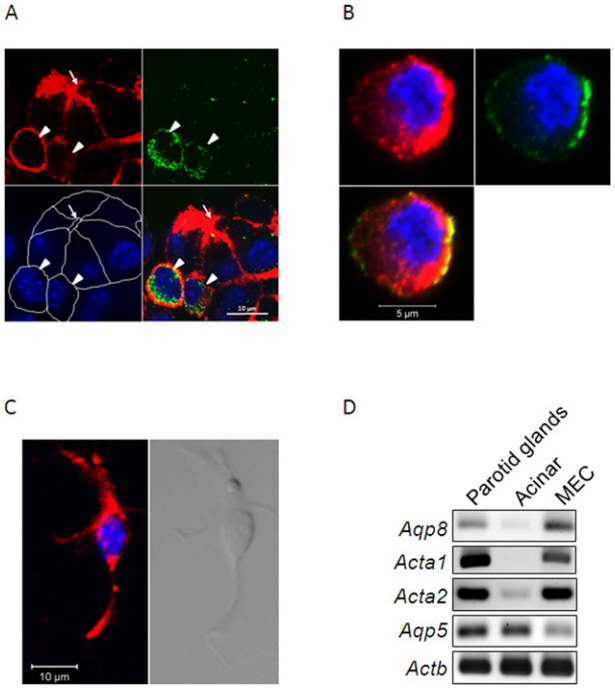


**Fig. 2.** Characterization of myoepithelial cells. Immunocytochemistry of acinar cells bound to myoepithelial cells before isolation by the density gradient centrifugation is seen in (A). Phalloidin staining (upper left), and immunostaining for aquaporin 8 (upper right); DAPI staining (lower left) shows white lines indicating cell edges. The merged image is shown in the lower right. Myoepithelial cells reactive to anti-aquaporin 8 were co-localized with phalloidin staining (arrow heads). An arrow indicates the lumen of the acinar cells. Double immunostaining was performed for actin-α1 (upper left) and aquaporin 8 (upper right) with DAPI staining of isolated myoepithelial cells (B). The typical shape of the myoepithelial cells re-emerged after isolation following paraformaldehyde fixation (C). Immunostaining with anti-actin-α1 (red) and DAPI (blue) staining are shown on the left; the transmission image is in the right. (D) RT-PCR of RNA prepared from the parotid glands, the isolated acinar cell fraction and the isolated myoepithelial cell fraction. *Aqp5*, which is reportedly expressed in acinar cells [18], was expressed in the acinar cell fraction but not in the myoepithelial cell fraction. *Aqp8* and *Acta1* were expressed in the myoepithelial cell fraction but not in the acinar cell fraction. (For interpretation of the references to color in this figure legend, the reader is referred to the web version of this article.)

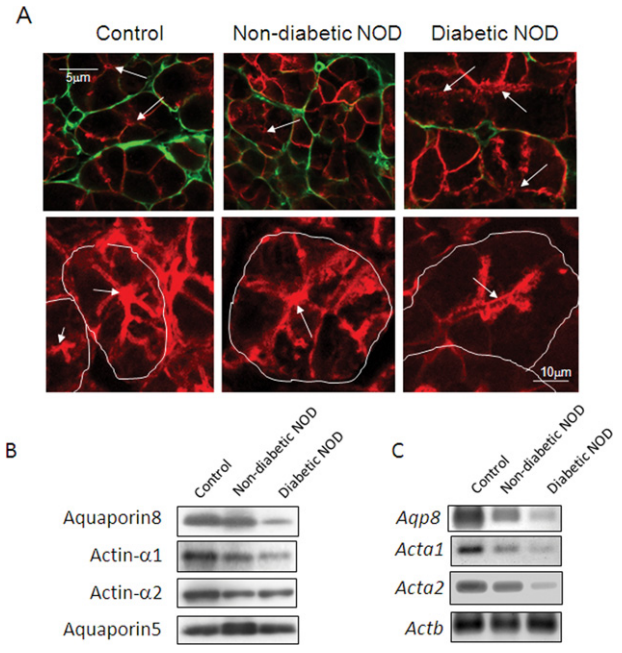


**Fig. 3.** Decreased marker signals in parotid glands of diabetic NOD mice. Immunohistochemistry of parotid glands from diabetic NOD mouse, non-diabetic NOD mouse and control mouse was performed with antibodies for anti-aquaporin 8 (A, upper panel). Distribution of aquaporin 8 (green) was shown with that of aquaporin 5 (red), as a marker for acinar cells [16]. Phalloidin staining is shown in the lower images; white lines indicate cell edges. Arrows indicate lumina of acinar cells. Homogenates were prepared from parotid glands of diabetic NOD mouse, non-diabetic NOD mouse and control mouse (C57BL/6), and analyzed by immunoblotting for myoepithelial cell markers; anti-actin-α1, anti-actin-α2, and anti-aquaporin 8 (B). Aliquots of homogenates (10 μg) were applied on a polyacrylamide gel plate. Actin-α1 was detected in control mouse parotid glands but rarely in diabetic NOD mouse parotid glands. RT-PCR was performed with 2.5 ng/μl template total RNA, prepared from parotid glands according to methods described under "Section 2" (C). Amplicons were amplified over 35 cycles. *Actb* (β-actin) was used as a positive internal standard. Data show a representative result from three repeat experiments in four animals. (For interpretation of the references to color in this figure legend, the reader is referred to the web version of this article.)

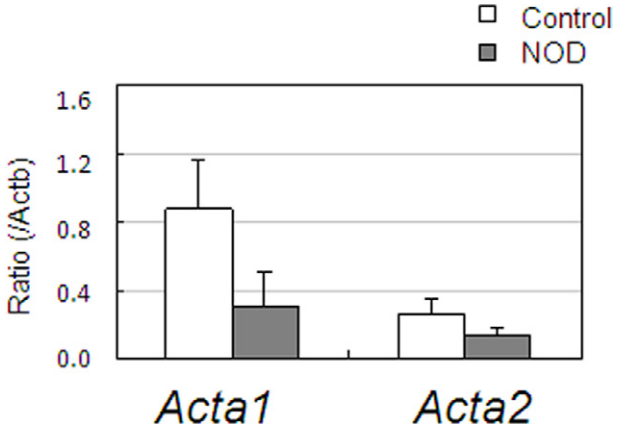


**Fig. 4.** Detection of myoepithelial cell components in diabetic mice using real-time quantitative PCR. Decreased *Acta1* and *Acta2* expression in parotid glands of diabetic NOD mice was defined by real-time quantitative PCR. Means and standard errors of values from four animals are shown. Statistical analysis was performed using unpaired Student's *t*-tests; significant differences were not detected, although *Acta1* and *Acta2* tended to have lower expression in diabetic mice.

contraction [13], but these roles are not well studied. Myoepithelial cells in mammary glands and those in salivary glands may have different characters; CD10 (CALLA, common acute lymphoblastic leukemia antigen), a marker of mammary myoepithelial cells, is reportedly not expressed in salivary glands [14]. The characters of these myoepithelial cells should be further compared.

Myoepithelial cells contain components of smooth muscle, including actin-α2, which is used as a marker [15], but is not specific for these cells [12]. Here, we isolated myoepithelial cells from mouse parotid glands; this investigation was our first attempt at salivary gland research. The isolated myoepithelial cells of parotid glands expressed mRNA transcripts of the skeletal muscle-related genes, *Acta1* (Fig. 2D), and were immunoreactive to actin-α1 antibody (Fig. 2B). The presence of skeletal muscle components in myoepithelial cells has not been reported. Epithelial cells are of mesodermal origin and contain smooth muscle, whereas, myoepithelial cells are of ectodermal origin, similar to that of sphincter pupillae muscle and iris dilator. Expression of the skeletal muscle components in myoepithelial cells may relate to their origin; by extension, further studies might find such skeletal muscle components in sphincter pupillae muscle and iris dilators. We would not expect to find other skeletal muscle components in the parotid glands, as shown in our experiments (Fig. 1C); therefore, actin-α1 and its mRNA could be used as markers for myoepithelial cells in the parotid glands.

In this study, we found that actin filaments outside acinar cells and expression of *Aqp8*, *Acta2* and *Acta1* genes decreased in parotid glands of diabetic NOD mice, indicating atrophy of myoepithelial cells in such mice. Quantitative real-time PCR confirmed that the expression of *Acta1* and *Acta2* in diabetic mice was also lower than that of controls. Our previous study of parotid glands from diabetic mice indicated increased interspaces between acinar cells [6]. Atrophy of myoepithelial cells may therefore increase the interspace in the parotid glands of diabetic NOD mice.

Loss of myoepithelial cells has been reported in sialadenosis patients [16]. Decrease of actin-α1, actin-α2 and aquaporin-8 may depend on the atrophy or destruction of myoepithelial cells caused by diabetes mellitus as a secondary phenomenon of sialadenosis. As the pathogenesis of xerostomia may include autoimmunity, diabetic NOD mice might develop pathologies in various tissues and salivary glands, similar to patients with Sjögren's syndrome [17]. The possible relationship between the pathology of Sjögren's syndrome and that of the model animals used here should be further investigated.

In conclusion, we have shown expression of *Acta*1, *Acta2* and *Aqp8*, and the proteins encoded by their mRNAs, were significantly reduced in parotid glands of diabetic mice compared with control mice. As non-diabetic NOD mice (which may be in pre-immune states) did not show the critical reduction, the altered protein and gene expressions might result from various etiologies, including immune responses, inflammation, or atrophy, as the near-final stage of tissue destruction, rather than the onset of diabetes. Fewer or atrophied myoepithelial cells in diabetic NOD mice imply the importance of these cells in salivary glands. Further investigation into their role is needed to define the mechanisms of onset of Sjögren's syndrome and its relationship to saliva secretion.

## Acknowledgements

We thank Dr. Hidekazu Aoyagi for his excellent technical assistance. This work was supported by Grants-in-Aid for Scientific Research Nos. 20592380 and 23592781 from the Japan Society for Promotion of Science.

## References

[1] Redman R.S. (1994) Myoepithelium of salivary glands. Microsc. Res. Tech. 27, 25–45.
[2] Ianez R.F., Buim M.E., Coutinho-Camillo C.M., Schultz R., Soares F.A., Lourenço S.V. (2010) Human salivary gland morphogenesis: myoepithelial cell maturation assessed by immunohistochemical markers. Histopathology. 57, 410–417.

[3] Ridgway W.M. (2006) Dissecting genetic control of autoimmunity in NOD congenic mice. Immunol. Res. 36, 189–195.
[4] Robinson C.P., Yamachika S., Alford C.E., Cooper C., Pichardo E.L., Shah N. et al. (1997) Elevated levels of cysteine protease activity in saliva and salivary glands of the nonobese diabetic (NOD) mouse model for Sjögren syndrome. Proc. Natl. Acad. Sci. U.S.A. 94, 5767–5771.
[5] Humphreys-Beher M.G. (1996) Animal models for autoimmune disease-associated xerostomia and xerophthalmia. Adv. Dent. Res. 10, 73–75.
[6] Fukushima T., Nashida T., Haga-Tsujimura M., Mataga I. (2012) Chitinase expression in parotid glands of non-obese diabetic mice. Oral Dis. 18, 506–512.
[7] Wellner R.B., Redman R.S., Swaim W.D., Baum B.J. (2006) Further evidence for AQP8 expression in the myoepithelium of rat submandibular and parotid glands. Pflugers Arch. 451, 642–645.
[8] Quissell D.O., Redman R.S. (1979) Functional characteristics of dispersed rat submandibular cells. Proc. Natl. Acad. Sci. U.S.A. 76, 2789–2793.
[9] Nashida T., Imai A., Yoshie S., Shimomura H., Yokosuka H., Kumakura M. (2008) Unstimulated amylase secretion is proteoglycan-dependent in rat parotid acinar cells. Arch. Biochem. Biophys. 469, 165–173.
[10] Clarke C., Titley J., Davies S., O'Hare M.J. (1994) An immunomagnetic separation method using superparamagnetic (MACS) beads for large-scale purification of human mammary luminal and myoepithelial cells. Epithelial Cell Biol. 3, 38–46.
[11] Moumen M., Chiche A., Cagnet S., Petit V., Raymond K., Faraldo M.M. et al. (2011) The mammary myoepithelial cell. Int. J. Dev. Biol. 55, 763–771.
[12] Ogawa Y. (2003) Immunocytochemistry of myoepithelial cells in the salivary glands. Prog. Histochem. Cytochem. 38, 343–426.
[13] Berggreen E., Wiig H. (2006) Lowering of interstitial fluid pressure in rat submandibular gland: a novel mechanism in saliva secretion. Am. J. Physiol. Heart Circ. Physiol. 290, H1460–H1468.
[14] Neves Cde O, Soares A.B., Costa A.F., de Araujo V.C., Furuse C., Juliano P.B. et al. (2010) CD10 (Neutral Endopeptidase) expression in myoepithelial cells of salivary neoplasms. Appl. Immunohistochem. Mol. Morphol. 18, 172–178.
[15] Miettinen M. (1988) Antibody specific to muscle actins in the diagnosis and classification of soft tissue tumors. Am. J. Pathol. 130, 205–215.
[16] Ihrler S., Rath C., Zengel P., Kirchner T., Harrison J.D., Weiler C. (2010) Pathogenesis of sialadenosis: possible role of functionally deficient myoepithelial cells. Oral Surg. Oral Med. Oral Pathol. Oral Radiol. Endod. 110, 218–223.
[17] Chiorini J.A., Cihakova D., Ouellette C.E., Caturegli P. (2009) Sjögren syndrome: advances in the pathogenesis from animal models. J. Autoimmun. 33, 190–196.
[18] Matsuzaki T., Suzuki T., Koyama H., Tanaka S., Takata K. (1999) Aquaporin-5 (AQP5), a water channel protein, in the rat salivary and lacrimal glands: immunolocalization and effect of secretory stimulation. Cell Tissue Res. 295, 513–521.